Oral Oncology 88 (2019) 1–8

Contents lists available at ScienceDirect

Oral Oncology

journal homepage: www.elsevier.com/locate/oraloncology

Perspectives

Accuracy of computer-assisted surgery in mandibular reconstruction: A postoperative evaluation guideline

Gustaaf J.C. van Baar[a,*], Niels P.T.J. Liberton[a], Tymour Forouzanfar[a], Henri A.H. Winters[b], Frank K.J. Leusink[a]

[a] Department of Oral and Maxillofacial Surgery/Oral Pathology & 3D Innovation Lab, VU University Medical Centre/Academic Centre for Dentistry Amsterdam (ACTA), De Boelelaan 1117, 1081 HV Amsterdam, the Netherlands
[b] Department of Plastic, Reconstructive and Hand Surgery, VU University Medical Centre, De Boelelaan 1117, 1081 HV Amsterdam, the Netherlands

ARTICLE INFO

Keywords:
Oral cancer
Mandibular reconstruction
Free tissue flaps
Surgery
Computer-assisted
Computer-aided design
Computer-aided manufacturing
Printing
Three-dimensional
Data accuracy
Software

ABSTRACT

Comparing accuracy results for mandibular reconstructions using computer-assisted surgery (CAS) is limited due to heterogeneity in image acquisition, extent of mandibular resection, and evaluation methodologies between studies. We propose a practical, feasible and reproducible guideline for standardizing evaluation methods to allow valid comparisons of postoperative results and facilitate meta-analyses in the future. It offers a guide to imaging, data comparison, volume assessment of 3-dimensional models, classification of defects, and it also contains a quantitative accuracy evaluation method.

Introduction

Mandibular reconstruction using computer-assisted surgery (CAS) involves planning, modeling, surgical [1,2], and evaluation phases [3–5]. In the planning phase, a computed tomography (CT) scan of the craniofacial skeleton and a CT (with or without angiography) of the donor site is obtained. These images consist of voxels with gray values proportional to the degree of x-ray attenuation of different tissue types, which are scaled according to Hounsfield units (HU) (air [−1000 HU], water [0 HU], and human bone [+1000 HU]) and saved as Digital Imaging and Communications in Medicine (DICOM) files. These DICOM images are converted into 3-dimensional (3D) surface models, a process requiring segmentation of the DICOM images into regions of interest (ROIs) [6]. The commonest segmentation method is thresholding: voxels with an HU above a selected threshold value are included in the ROI and transformed into 3D surface models in the Standard Tessellation Language (STL) file format [7]. These STL models can be imported into computer-aided design software to construct 3D guides [8]. In the modeling phase, the virtually planned 3D guides are printed and subsequently used in the surgical phase [8]. In the evaluation, a CT scan of the patient's craniofacial skeleton is repeated and pre- and postoperative data sets are compared.

Our recently published systematic review on accuracy of computer-assisted surgery in mandibular reconstruction demonstrated a lack of uniformity in image acquisition, mandibular defect classification, and evaluation methodologies. This heterogeneity limits valid comparisons of postoperative results between studies [9]. However, the new European Union medical device regulation (MDR) obliges standardization and Conformité Européenne (CE) certification for CAS processes and enter into force on spring 2020 [10].

We propose a practical, feasible and reproducible evaluation guideline to create uniformity in studies regarding the postoperative evaluation of mandibular reconstructions using CAS and facilitate meta-analyses in the future.

Abbreviations: CAS, computer-assisted surgery; CT, computed tomography; MDCT, multiple detector computed tomography; HU, Hounsfield units; DICOM, Digital Imaging and Communications in Medicine; ROI, region of interest; STL, Standard Tessellation Language

* Corresponding author at: Room ZH 1B-05, De Boelelaan 1117, 1081 HZ Amsterdam, the Netherlands.
E-mail addresses: g.vanbaar@vumc.nl (G.J.C. van Baar), n.liberton@vumc.nl (N.P.T.J. Liberton), t.forouzanfar@vumc.nl (T. Forouzanfar), h.winters@vumc.nl (H.A.H. Winters), f.leusink@vumc.nl (F.K.J. Leusink).

https://doi.org/10.1016/j.oraloncology.2018.11.013
Received 3 September 2018; Received in revised form 7 November 2018; Accepted 9 November 2018
Available online 16 November 2018

Evaluation guideline

All steps in this guideline should be independently validated by at least two different observers.

Imaging

Inaccuracies caused by quality of CT data and differences in quality between pre- and postoperative CT data should be minimized [9]. Therefore, pre- and postoperative imaging should be performed with multiple detector CT (MDCT) using the identical machine and scanner parameters. Slice thickness is the most influencing factor in volume measurements and should be set < 1.25 mm [11,12]. The postoperative MDCT scan should be performed within six weeks to create uniformity in the postoperative evaluation between studies, and to bypass long-term changes in the volume or position of the segments of bone graft [13]. If adjuvant radiation therapy is indicated, the first postoperative MDCT scan prior to the radiation should be used to bypass radiation-related pathology in the mandibular bone [14].

Classification of mandibular defects

Classify the mandibular defect according to the classification of Brown et al. [15] to facilitate comparisons between similar reconstructions.

STL volume assessment

Pre- and postoperative STL models should be checked on similarity by superimposing a certain part of the remnant mandible of the preoperative STL model (not in touch with the metal fixation) on the postoperative STL model, or vice versa. The software can subsequently calculate the volume discrepancy expressed in an arithmetic mean in mm (Fig. 1). In case of an arithmetic mean > 0.5 mm [16], the postoperative MDCT scan segmentation should be repeated by adjusting the threshold values.

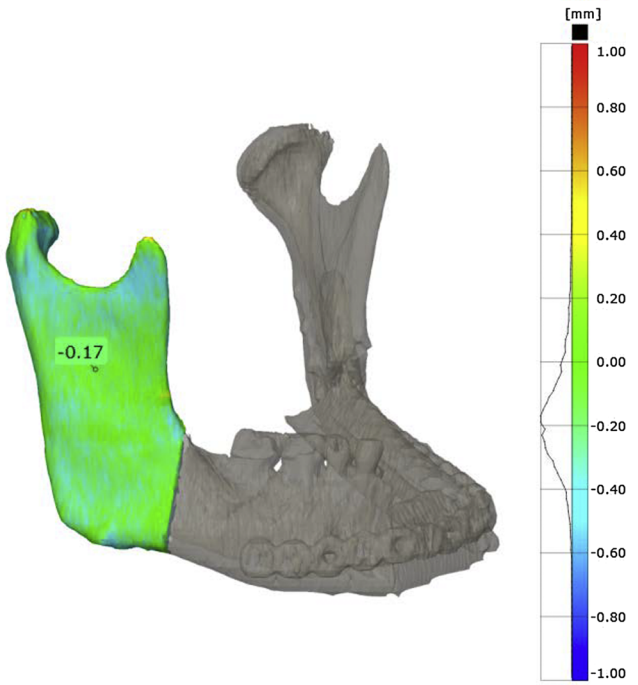

Fig. 1. Example of the STL volume assessment: a part of the remnant mandible (not in touch with the metal fixation) of the preoperative STL model is superimposed on the postoperative STL model. The arithmetic mean in this example is 0.17 mm, which is accurate enough (< 0.5 mm) to continue to the next step in the evaluation guideline.

XYZ orientation

The Frankfurt plane, midsagittal plane, and the nasion should be used for XYZ orientation of the preoperative STL model (revised to the virtual plan). The Frankfurt plane is determined by drawing a plane passing both internal acoustic foramen and the left infraorbital margin [17]. The midsagittal plane is determined by drawing a plane passing the nasion, basion and the incisive foramen [18]. A plane-line-point software tool should be used to position the skull on the XYZ-axis, projecting the Frankfurt plane to the Z-axis (plane), the midsagittal plane to the Y-axis (line), and the nasion to the X-axis (point).

Superimposition of the condylar processes

The postoperative STL model of the entire reconstruction should be superimposed on the preoperative STL model (revised to the virtual plan), with only both condylar processes selected for the iterative closest-point algorithm. This is done by selecting both condylar processes on the postoperative STL model by drawing a plane from the most caudal point of the incisura mandibulae (mandibular notch) perpendicular to the posterior edge of the border between condyle and ramus (Fig. 2).

Calculation of the right and left axial, coronal, and sagittal mandibular angles

To prevent bias, the postoperative STL model should be deselected during the identification of bony landmarks in the preoperative STL model, and vice versa. Virtual points are determined on the most superior and posterior part of the condyle. In case of a vertical segment of bone graft or a titanium/prosthetic condyle, these virtual points are located on the most superior- and posterior parts. The vertical corner and horizontal corner according to the classification of Brown et al. are identified. If a corner is included in the resection, the most inferior point of the osteotomy plane between the two segments of bone graft should be selected. When half of a corner is included in the resection (remnant mandible adjacent to a segment of bone graft), the most inferior point of the osteotomy plane on the segment of bone graft should be selected. In class I defects a virtual point on the most anterior and inferior part of the horizontal segment of bone graft should be created and considered as horizontal corner. When the surgeon prefers osteotomies outside the anatomical corners, the osteotomy closest to the anatomical corner should be identified as vertical- or horizontal corner.

Subsequently, using these four bony landmarks (the condyle superior, condyle posterior, vertical corner and horizontal corner) and the midsagittal line, the right and left mandibular angles (°) can be calculated:

- The coronal mandibular angles are calculated between the lines from condyle superior to vertical corner and the midsagittal line.
- The axial mandibular angles are calculated between the lines from vertical corner to horizontal corner and the midsagittal line.
- The sagittal mandibular angles are calculated between the lines from condyle posterior to vertical corner and the lines from vertical corner to horizontal corner.

Differences between the postoperative angles and the virtual planned angles should be calculated and reported.

Calculation of the xyz deviations of the dental implants

The correct dental implant diameter and height (including the cover screw) should be used in the preoperative planning for correct comparison. Using the zero reference point on the XYZ-axis (previously

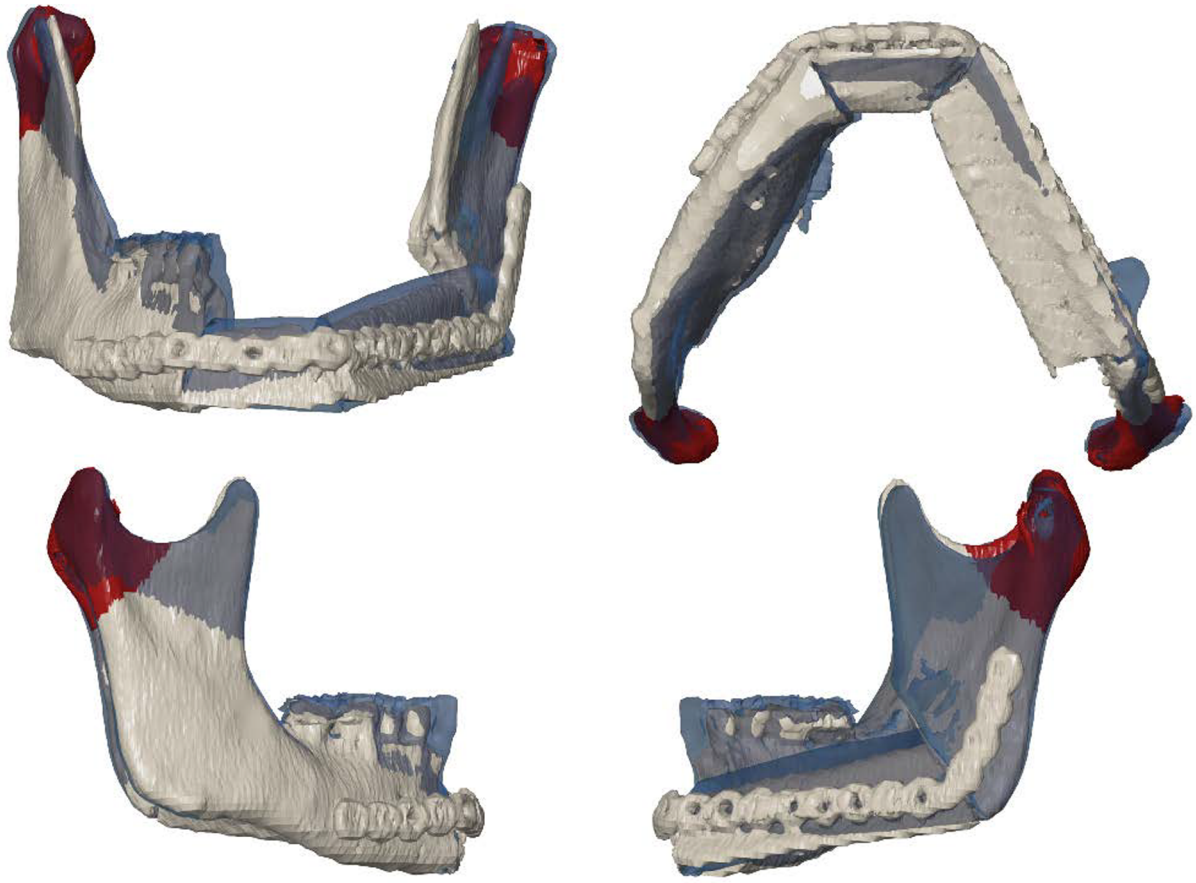

Fig. 2. Example of the superimposition of the condylar processes: the postoperative STL model of the entire mandibular reconstruction is superimposed on the preoperative STL model (revised to the virtual plan), with only both condylar processes selected for the iterative closest-point algorithm (shown in red).

created during step 4), the XYZ- axis position of the top of the dental implant in the middle of the cover screw is measured with a XYZ-deviation plot tool in the pre- and postoperative STL models. Subsequently, the differences on the X-, Y- and Z-axis in mm are calculated by subtracting the preoperative XYZ-values (x_1, y_1 and z_1) from the postoperative XYZ-values (x_2, y_2 and z_2). The dental implant distance XYZ (dXYZ) from point to point (virtual planning vs. postoperative result in mm) should be calculated with the formula:

$$dXYZ = \sqrt{(x^2 - x^1)^2 + (y^2 - y^1)^2 + (z^2 - z^1)^2}$$

How to use this evaluation guideline

As an example for the use of this guideline, three cases from our department including a Brown class I, class II and class III reconstruction are evaluated in Figs. 3–5.

Discussion

Postoperative hard tissue accuracy of mandibular reconstructions using CAS should be evaluated by four components: (1) the position of the condyles, (2) the angles of the osteotomy planes, (3) the position and size of the segments of the bone graft, and (4) the position of the dental implants.

De Maesschalck et al. described an evaluation method to measure hard tissue accuracy, which bypasses the difficult determination of osteotomy planes by calculating the differences in linear and angular parameters on pre- and postoperative STL models [19]. However, de Maesschalck does not use a standardized and reproducible method to determine the midsagittal plane, virtually planned dental implants are not included in the evaluation method, and no attempt is made to differentiate between complexity of mandibular reconstructions.

A mandibular defect classification is required to categorize the complexity of mandibular reconstructions and thereby facilitate comparisons between similar reconstructions. Brown et al. proposed a classification based on the principle that the mandible has four corners: two vertical corners (mandibular angles) and two horizontal corners (in the dentate mandible centered at the canine teeth on each side and in the edentate mandible approximately 7 mm anterior to the mental foramen). These four corners correlate with the need to shape a bone graft with osteotomies. Brown et al. describes four classes: class I (angle), class II (angle and canine), class III (both canines, no angles), and class IV (both canines and at least one angle). A “c” is added if the condyle is involved. Mandibular defects not including a vertical- or horizontal corner(s) are classified according to the closest corner. The higher the defect class, the higher the complexity of the reconstruction [15].

In our proposed guideline, we defined lines between the condyle, vertical- and horizontal corner (according to the classification of Brown et al.) and subsequently created axial, coronal, and sagittal mandibular angles (pioneered by de Maesschalk et al. [19]). Additional, an evaluation method of the postoperative positions of virtually planned dental implants are included. CAS facilitates dental implant placement at the time of initial reconstruction in line with the antagonist dentition [20,21], with higher utilization of implants and shorter time to complete dental rehabilitation [22,23]. The number of authors applying this technique in the future is likely to increase. The postoperative position of the neck of the dental implant is important with regard to the future dental rehabilitation. Angular deviations up to 15° are not a major concern since angled abutments can help to correct these deviations.

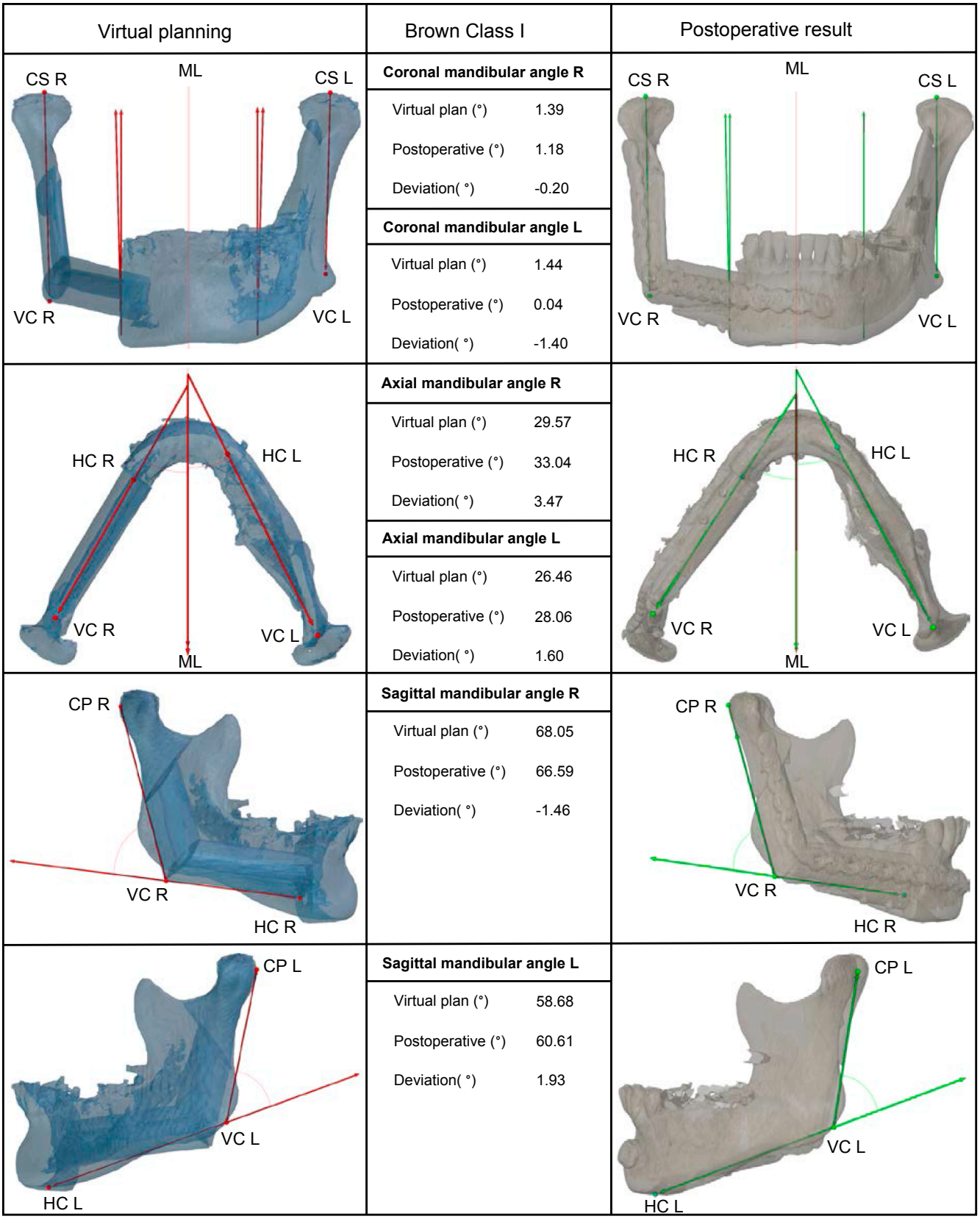

Fig. 3. Example of a Class I reconstruction according to Brown et al. [15] evaluated according to the proposed guideline. Coronal, axial and sagittal angles of the virtual planning and the postoperative result are shown and compared. The patient had a normal postoperative occlusion. CS, condyle superior; CP, condyle posterior; VC, vertical corner; HC, horizontal corner; ML, midsagittal line.

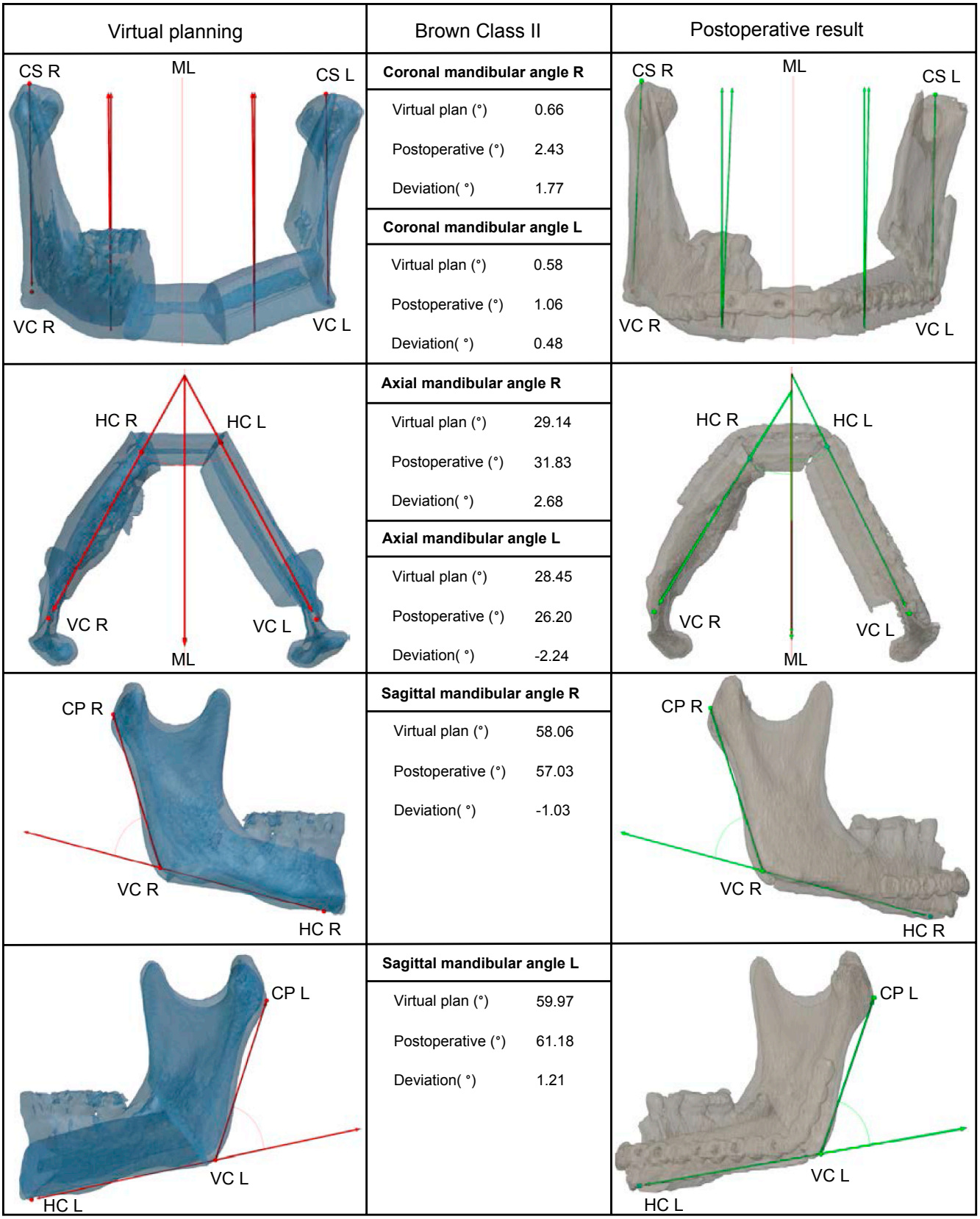

Brown Class II		
Coronal mandibular angle R		
Virtual plan (°)	0.66	
Postoperative (°)	2.43	
Deviation(°)	1.77	
Coronal mandibular angle L		
Virtual plan (°)	0.58	
Postoperative (°)	1.06	
Deviation(°)	0.48	
Axial mandibular angle R		
Virtual plan (°)	29.14	
Postoperative (°)	31.83	
Deviation(°)	2.68	
Axial mandibular angle L		
Virtual plan (°)	28.45	
Postoperative (°)	26.20	
Deviation(°)	-2.24	
Sagittal mandibular angle R		
Virtual plan (°)	58.06	
Postoperative (°)	57.03	
Deviation(°)	-1.03	
Sagittal mandibular angle L		
Virtual plan (°)	59.97	
Postoperative (°)	61.18	
Deviation(°)	1.21	

Fig. 4. Example of a Class II reconstruction according to Brown et al. [15] evaluated according to the proposed guideline. Coronal, axial and sagittal angles of the virtual planning and the postoperative result are shown and compared. The patient had a normal postoperative occlusion. CS, condyle superior; CP, condyle posterior; VC, vertical corner; HC, horizontal corner; ML, midsagittal line.

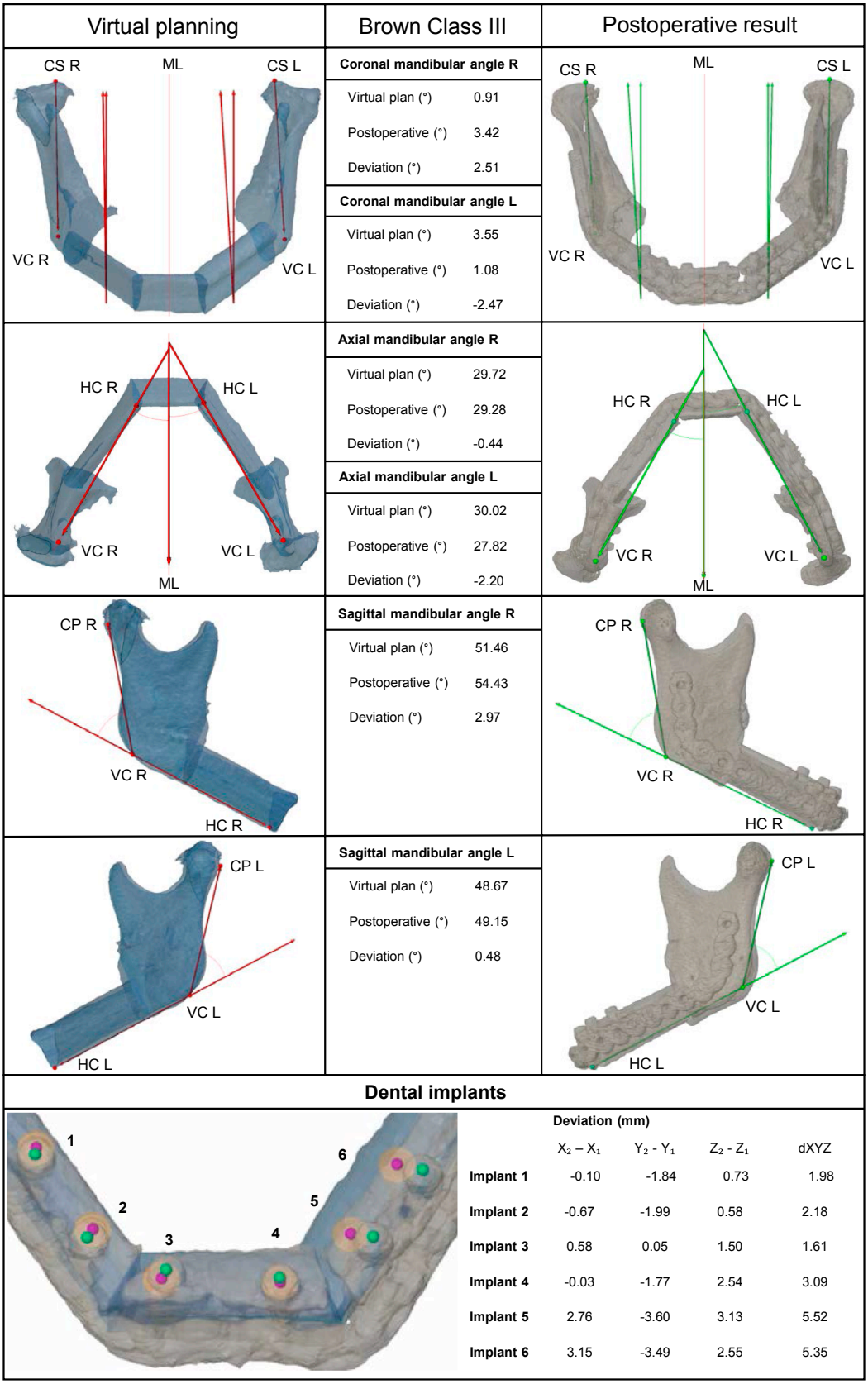

Fig. 5. Example of a Class III reconstruction according to Brown et al. [15] with virtually planned dental implants, evaluated according to the proposed guideline. Coronal, axial and sagittal angles of the virtual planning and the postoperative result are shown and compared. Dental implant deviations on the X-, Y- and Z-axis and the point-to-point distance XYZ (dXYZ) per implant are shown. Post-operatively there was no occlusion according to the virtual plan. CS, condyle superior; CP, condyle posterior; VC, vertical corner; HC, horizontal corner; ML, midsagittal line.

Tarsitano et al. published an evaluation method for mandibular reconstruction using CAS [24]. A few considerations should be highlighted: (1) An evaluation method for virtually planned dental implants should be included. (2) Accuracy results were published as 'average error' in mm, therefore the origin of inaccuracies is not traceable. (3) Alignment of the pre- and postoperative STL models was performed by superimposition of the entire mandibular reconstruction. This software tool calculates the most favorable correspondence ('best fit') of two clouds of points with an iterative closest-point algorithm. Hence, superimposing the postoperative STL model of the entire reconstruction (including potential inaccuracies) allows deviations to 'best fit' the preoperative STL model of the virtual plan, not taking into account the postoperative intermaxillary relationship and position of the condyles. Another reason why superimposing the entire reconstruction is not recommended is the scattering caused by the fixation plate(s), introducing inaccuracies in the alignment of STL models [25–27].

The alignment of pre- and postoperative STL models is complicated because of confounders affecting the postoperative mandibular position relative to the cranium and maxilla (e.g. temporomandibular joint hydrops, differences in mouth-opening between pre- and postoperative CT scans, and the unpredictability of the postoperative intermaxillary relation due to the unpredictable position of the condyles relative to the fossae). Difficulties arise when studies attempt to implement the superimposition tool: (1) superimposition of the full reconstructed mandible is discouraged because of the intermaxillary deviations and scattering of the fixation plate(s), (2) superimposition of isolated parts of the neomandible (e.g., segments of bone graft, reconstruction plate, dental implants) is discouraged due to deviations relative to the entire reconstruction, and (3) superimposition of the cranial region is discouraged due to the confounding factors affecting the postoperative mandibular position.

In our opinion, superimposition of both condylar processes is the most simple, reliable and reproducible method for pre- and postoperative STL model alignment. The postoperative condyle position can be affected by incorrect position and placement of the neomandible [28]. However, CAS techniques showed increased reproducibility of virtually planned positioning of the condyles [2,28]. In case of condyle deviation, the intermaxillary relation starts to adapt to the midline and subsequently averages the position of both condyles around the midsagittal plane. This modification was noted by Hidalgo et al. as: "tandem temporomandibular joint function across the midline", and called "a unique property of the mandible" [29]. Fortuitously, this averaging around the midsagittal plane is comparable to superimposition of both condylar processes. In case of a resected condyle, the condyle is substituted by a vertical segment of bone graft or a custom titanium reconstruction plate including a titanium/prosthetic condyle [29,30]. Both still can be used for superimposition by selecting a surface of similar volume compared to the opposite condylar process. A systematic review on mandibular reconstruction with vascularized bone flaps of Brown et al. showed that the condyle is resected in only 10% of all cases [31].

Mandibular reconstructions are frequently exposed to postoperative adjuvant therapy with potential consequences for the (neo)mandibular bone. Radiation-related pathology in mandibular bone (i.e. atrophy, non-union, osteoradionecrosis and fractures) could potentially influence the long-term volume and positioning of the segments of bone graft [13]. Radiation therapy (if indicated) usually starts within six weeks after surgery and is preceded by a postoperative MDCT scan, which can be used simultaneously to evaluate postoperative accuracy outcomes [14]. Further research could be conducted to determine the influence of radiation therapy on the (neo)mandibular bone using our proposed evaluation guideline.

Tolerable outcome ranges in mandibular reconstruction using CAS and their consequences for functional outcome are lacking in studies reviewed so far [9,19]. Our evaluation guideline could contribute to a much more systematic and uniform approach to objectify these relationships. Acceptable coronal, axial and sagittal angle deviations, their relationship with the postoperative positions of dental implants, and acceptable dental implant deviations (dXYZ) need to be determined in future research. It is important to bear in mind that outcome ranges are separated per Brown class and preferably should be related to functional outcome. To do so, our department will conduct a multicenter validation study, which takes all the above mentioned variables into account.

Conclusion

Our evaluation guideline offers a guide to imaging, classification of defects, data comparison, and volume assessment of 3D models. Furthermore, it contains a quantitative accuracy evaluation method.

Conflict of interest

None declared.

Acknowledgements

This research did not receive any specific grant from funding agencies in the public, commercial, or not-for-profit sectors.

References

[1] Hirsch DL, Garfein ES, Christensen AM, Weimer KA, Saddeh PB, Levine JP. Use of computer-aided design and computer-aided manufacturing to produce orthognathically ideal surgical outcomes: a paradigm shift in head and neck reconstruction. J Oral Maxillofac Surg 2009;67(10):2115–22.
[2] Ciocca L, Mazzoni S, Fantini M, Persiani F, Baldissara P, Marchetti C, et al. A CAD/CAM-prototyped anatomical condylar prosthesis connected to a custom-made bone plate to support a fibula free flap. Med Biol Eng Comput 2012;50(7):743–9.
[3] Rodby KA, Turin S, Jacobs RJ, Cruz JF, Hassid VJ, Kolokythas A, et al. Advances in oncologic head and neck reconstruction: systematic review and future considerations of virtual surgical planning and computer aided design/computer aided modeling. J Plast Reconstr Aesthet Surg 2014;67(9):1171–85.
[4] Shu DL, Liu XZ, Guo B, Ran W, Liao X, Zhang YY. Accuracy of using computer-aided rapid prototyping templates for mandible reconstruction with an iliac crest graft. World J Surg Oncol 2014;12:190.
[5] Succo G, Berrone M, Battiston B, Tos P, Goia F, Appendino P, et al. Step-by-step surgical technique for mandibular reconstruction with fibular free flap: application of digital technology in virtual surgical planning. Eur Arch Otorhinolaryngol 2015;272(6):1491–501.
[6] Rengier F, Mehndiratta A, von Tengg-Kobligk H, Zechmann CM, Unterhinninghofen R, Kauczor HU, et al. 3D printing based on imaging data: review of medical applications. Int J Comput Assist Radiol Surg 2010;5(4):335–41.
[7] Marro A, Bandukwala T, Mak W. Three-dimensional printing and medical imaging: A review of the methods and applications. Curr Probl Diagn Radiol 2016;45(1):2–9.
[8] Mitsouras D, Liacouras P, Imanzadeh A, Giannopoulos AA, Cai T, Kumamaru KK, et al. Medical 3D printing for the radiologist. Radiographics 2015;35(7):1965–88.
[9] van Baar GJC, Forouzanfar T, Liberton N, Winters HAH, Leusink FKJ. Accuracy of computer-assisted surgery in mandibular reconstruction: A systematic review. Oral Oncol 2018;84:52–60.
[10] Regulation (EU) 2017/745 of the European Parliament and of the Council of 5 April 2017 on medical devices, amending Directive 2001/83/EC, Regulation (EC) No 178/2002 and Regulation (EC) No 1223/2009 and repealing Council Directives 90/385/EEC and 93/42/EEC Official Journal of the European Union 2017;60(117):1–332.
[11] Whyms BJ, Vorperian HK, Gentry LR, Schimek EM, Bersu ET, Chung MK. The effect of computed tomographic scanner parameters and 3-dimensional volume rendering techniques on the accuracy of linear, angular, and volumetric measurements of the mandible. Oral Surg Oral Med Oral Pathol Oral Radiol 2013;115(5):682–91.
[12] Taft RM, Kondor S, Grant GT. Accuracy of rapid prototype models for head and neck reconstruction. J Prosthet Dent 2011;106(6):399–408.
[13] Disa JJ, Winters RM, Hidalgo DA. Long-term evaluation of bone mass in free fibula flap mandible reconstruction. Am J Surg 1997;174(5):503–6.
[14] Jereczek-Fossa BA, Orecchia R. Radiotherapy-induced mandibular bone complications. Cancer Treat Rev 2002;28(1):65–74.
[15] Brown JS, Barry C, Ho M, Shaw R. A new classification for mandibular defects after oncological resection. Lancet Oncol 2016;17(1):e23–30.
[16] van Eijnatten M, Koivisto J, Karhu K, Forouzanfar T, Wolff J. The impact of manual threshold selection in medical additive manufacturing. Int J Comput Assist Radiol Surg 2017;12(4):607–15.
[17] Pittayapat P, Jacobs R, Bornstein MM, Odri GA, Lambrichts I, Willems G, et al. Three-dimensional Frankfort horizontal plane for 3D cephalometry: a comparative assessment of conventional versus novel landmarks and horizontal planes. Eur J Orthod 2018;40(3):239–48.

[18] Green MN, Bloom JM, Kulbersh R. A simple and accurate craniofacial midsagittal plane definition. Am J Orthod Dentofacial Orthop 2017;152(3):355–63.
[19] De Maesschalck T, Courvoisier DS, Scolozzi P. Computer-assisted versus traditional freehand technique in fibular free flap mandibular reconstruction: a morphological comparative study. Eur Arch Otorhinolaryngol 2017;274(1):517–26.
[20] Avraham T, Franco P, Brecht LE, Ceradini DJ, Saadeh PB, Hirsch DL, et al. Functional outcomes of virtually planned free fibula flap reconstruction of the mandible. Plast Reconstr Surg 2014;134(4):628e–34e.
[21] Schepers RH, Raghoebar GM, Vissink A, Lahoda LU, Van der Meer WJ, Roodenburg JL, et al. Fully 3-dimensional digitally planned reconstruction of a mandible with a free vascularized fibula and immediate placement of an implant-supported prosthetic construction. Head Neck 2013;35(4):E109–14.
[22] Anne-Gaelle B, Samuel S, Julie B, Renaud L, Pierre B. Dental implant placement after mandibular reconstruction by microvascular free fibula flap: current knowledge and remaining questions. Oral Oncol 2011;47(12):1099–104.
[23] Chuka R, Abdullah W, Rieger J, Nayar S, Seikaly H, Osswald M, et al. Implant utilization and time to prosthetic rehabilitation in conventional and advanced fibular free flap reconstruction of the maxilla and mandible. Int J Prosthodont 2017;30(3):289–94.
[24] Tarsitano A, Battaglia S, Ricotta F, Bortolani B, Cercenelli L, Marcelli E, et al. Accuracy of CAD/CAM mandibular reconstruction: A three-dimensional, fully virtual outcome evaluation method. J Craniomaxillofac Surg 2018;46(7):1121–5.
[25] Hanken H, Schablowsky C, Smeets R, Heiland M, Sehner S, Riecke B, et al. Virtual planning of complex head and neck reconstruction results in satisfactory match between real outcomes and virtual models. Clin Oral Investig 2015;19(3):647–56.
[26] Roser SM, Ramachandra S, Blair H, Grist W, Carlson GW, Christensen AM, et al. The accuracy of virtual surgical planning in free fibula mandibular reconstruction: comparison of planned and final results. J Oral Maxillofac Surg 2010;68(11):2824–32.
[27] Schepers RH, Raghoebar GM, Vissink A, Stenekes MW, Kraeima J, Roodenburg JL, et al. Accuracy of fibula reconstruction using patient-specific CAD/CAM reconstruction plates and dental implants: A new modality for functional reconstruction of mandibular defects. J Craniomaxillofac Surg 2015;43(5):649–57.
[28] Sawh-Martinez R, Parsaei Y, Wu R, Lin A, Metzler P, DeSesa C, et al. Improved temporomandibular joint position after 3-dimensional planned mandibular reconstruction. J Oral Maxillofac Surg 2017;75(1):197–206.
[29] Hidalgo DA, Pusic AL. Free-flap mandibular reconstruction: a 10-year follow-up study. Plast Reconstr Surg 2002;110(2):438–49. discussion 50–1.
[30] Kakarala K, Shnayder Y, Tsue TT, Girod DA. Mandibular reconstruction. Oral Oncol 2018;77:111–7.
[31] Brown JS, Lowe D, Kanatas A, Schache A. Mandibular reconstruction with vascularised bone flaps: a systematic review over 25 years. Br J Oral Maxillofac Surg 2017;55(2):113–26.